J|A|C|S ARTICLES

Published on Web 08/04/2010

Engineering of the Heme Pocket of an H-NOX Domain for Direct Cyanide Detection and Quantification

Zhou Dai and Elizabeth M. Boon*

Department of Chemistry, Stony Brook University, Stony Brook, New York 11794-3400

Received February 26, 2010; E-mail: elizabeth.boon@stonybrook.edu

Abstract: A new cyanide sensing system, the Heme-Nitric oxide and/or OXygen binding domain (H-NOX domain) from *Thermoanaerobacter tengcongensis* (*Tt* H-NOX), has been investigated. With straightforward absorbance-based detection, we have achieved a cyanide detection limit of 0.5 μM (~10 ppb) with an upper detection range that is adjustable with protein concentration. We find a linear correlation of multiple spectroscopic features with cyanide concentration. These spectroscopic features include the Soret band maximum and absorbance changes in both the Soret and α/β band regions of the spectrum. Multiple probes for cyanide detection makes sensing with *Tt* H-NOX unique compared to other cyanide sensing methods. Furthermore, using site-directed mutagenesis, we have rationally engineered the heme pocket of *Tt* H-NOX to improve its cyanide sensing properties. Using a mutant that alters the heme structure of *Tt* H-NOX (P115A) we were able to introduce colorimetric detection of cyanide. Through substituting phenylalanine 78 with a smaller (valine, F78V) or a larger residue (tyrosine, F78Y), we demonstrate a correlation with distal pocket steric crowding and affinity for cyanide. In particular, F78V *Tt* H-NOX shows a significant increase in CN^- binding affinity and selectivity. Thus, we demonstrate the ability to fine-tune the affinity and specificity of *Tt* H-NOX for cyanide, suggesting that *Tt* H-NOX can be readily tailored into a practical cyanide sensor.

Introduction

Cyanide is well-known for its extreme toxicity to mammals, due to its ability to bind to the active site of cytochrome oxidase and inhibit cellular respiration.[1] Cyanide poisoning can lead to vomiting, convulsions, unconsciousness, and most severely, death. However, cyanide is still widely used in industrial fields, including electroplating, metal mining, and plastic manufacture. Accidental leaks and spills of cyanide can lead to disastrous consequences.[2] Therefore, it is highly desirable to develop safe, simple, and direct sensing techniques for cyanide detection and quantification.

As suggested by the World Health Organization, the maximum acceptable level of cyanide in drinking water is 1.9 μM.[3] Thus, numerous analytical techniques have been developed to detect and quantify cyanide at submicromolar concentrations. Probes including silver electrodes,[4] boronic acids,[5] cationic boranes,[6,7] cobalt corrinoids,[8,9] benzil,[10] coumarin with a salicylaldehyde moiety,[11] acridinium salt,[12] and oxazines,[13,14] have been used in amperometric, chromatographic, fluorometric, and colorimetric assays for cyanide detection.[4−22] These systems, however, either require sophisticated equipment and/or laborious sample pretreatment, or are subject to interference by other anions.[4,22] Additionally, some of the cyanide detectors are organic materials that require laborious synthesis and usually have poor water solubility.[12,19] Although efforts have been made to design cyanide sensors that function in aqueous solution, a certain percentage of organic solvent is often required in the detection media for those organic probes.[6,10,12,15,19] Thus, new water-soluble cyanide detection techniques with high sensitivity and selectivity, that are easily accessed without relying on complicated analytical processes, are desired. Here, we introduce a new cyanide sensing system: the Heme-Nitric oxide and/or

(1) Vennesland, B.; Conn, E. E.; Knownles, C. J.; Westly, J.; Wissing, F. *Cyanide in Biology*; Academic Press: London, 1981.
(2) Koenig, R. *Science* **2000**, *287*, 1737.
(3) *Guidelines for Drinking-Water Quality*; World Health Organization: Geneva, 1996.
(4) Weinberg, H. S.; Cook, S. *J. Anal. Chem.* **2002**, *74*, 6055.
(5) Badugu, R.; Lakowicz, J. R.; Geddes, C. D. *J. Am. Chem. Soc.* **2005**, *127*, 3635.
(6) Hudnall, T. W.; Gabbaï, F. P. *J. Am. Chem. Soc.* **2007**, *129*, 11978.
(7) Kim, Y.; Zhao, H.; Gabbaï, F. P. *Angew. Chem., Int. Ed.* **2009**, *48*, 4957.
(8) Männel-Croisé, C.; Zelder, F. *Inorg. Chem.* **2009**, *48*, 1272.
(9) Zelder, F. H. *Inorg. Chem.* **2008**, *47*, 1264.
(10) Cho, D.-G.; Kim, J. H.; Sessler, J. L. *J. Am. Chem. Soc.* **2008**, *130*, 12163.
(11) Lee, K.-S.; Kim, H.-J.; Kim, G.-H.; Shin, I.; Hong, J.-I. *Org. Lett.* **2007**, *10*, 49.
(12) Yang, Y.-K.; Tae, J. *Org. Lett.* **2006**, *8*, 5721.
(13) Tomasulo, M.; Raymo, F. M. *Org. Lett.* **2005**, *7*, 4633.
(14) Tomasulo, M.; Sortino, S.; White, A. J. P.; Raymo, F. M. *J. Org. Chem.* **2005**, *71*, 744.
(15) Chow, C.-F.; Lam, M. H. W.; Wong, W.-Y. *Inorg. Chem.* **2004**, *43*, 8387.
(16) Gettler, A. O.; Goldbaum, L. *Anal. Chem.* **2002**, *19*, 270.
(17) Guilbault, G. G.; Kramer, D. N. *Anal. Chem.* **2002**, *37*, 1395.
(18) Mottola, H. A.; Freiser, H. *Anal. Chem.* **2002**, *40*, 1266.
(19) Peng, L.; Wang, M.; Zhang, G.; Zhang, D.; Zhu, D. *Org. Lett.* **2009**, *11*, 1943.
(20) Poland, K.; Topoglidis, E.; Durrant, J. R.; Palomares, E. *Inorg. Chem. Commun.* **2006**, *9*, 1239.
(21) Shan, D.; Mousty, C.; Cosnier, S. *Anal. Chem.* **2004**, *76*, 178.
(22) Smit, M. H.; Cass, A. E. G. *Anal. Chem.* **1990**, *62*, 2429.

10.1021/ja101674z

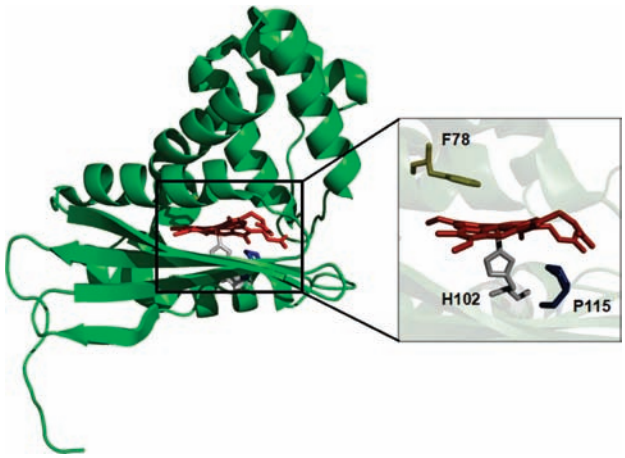

Figure 1. Crystal structure of *Tt* H-NOX (PDB 1U55). P115, F78, and H102 residues are colored in blue, yellow and gray, respectively.

OXygen binding domain (H-NOX domain) from *Thermoanaerobacter tengcongensis* (*Tt* H-NOX).[23]

It is well established that cyanide binds to hemoproteins and induces absorbance changes to the UV/visible spectra of the protein. Nonetheless, *Tt* H-NOX has many intriguing features that make it a unique new candidate for a cyanide sensor. H-NOX proteins are a family of recently discovered diatomic gas binding and sensing hemoproteins that are highly homologous to soluble guanylate cyclase (sGC), the well-studied nitric oxide (NO) sensor in eukaryotes.[24] The *Tt* H-NOX domain has been well characterized: (1) the crystal structure of wildtype (WT) *Tt* H-NOX has been solved to a resolution of 1.77 Å (Figure 1);[23] (2) it can be easily overexpressed and purified;[25] (3) it is very soluble in water; (4) as it was isolated from a thermophilic bacterium living at 75 °C, it is extremely stable at room temperature and can tolerate high temperatures; (5) its fold is tolerant of mutagenesis;[26,27] (6) its ferric state binds cyanide very tightly, while its ferrous state shows no affinity for cyanide;[28] and (7) the heme of *Tt* H-NOX can be easily converted between ferrous and ferric states, which should facilitate its use as a reusable cyanide indicator. Furthermore, mutants of *Tt* H-NOX have already been proven to be robust protein sensors of small molecules; Y140F *Tt* H-NOX has been used as a nitric oxide sensor.[29]

In this work, we have explored the application of *Tt* H-NOX as a sensitive and specific cyanide sensor in an assay based on UV/visible absorbance changes. *Tt* H-NOX senses CN^- with a detection limit of 0.5 μM (at the level of 10 ppb), which is much more sensitive than recently reported optical sensor based on hemoglobin (~0.2 ppm).[20] We demonstrate that the well-characterized *Tt* H-NOX P115A mutant has improved CN^- sensing properties, in particular, affording increased anion selectivity and colorimetric detection. On the basis of a comparison of WT and P115A *Tt* H-NOX, we develop a model relating heme distal pocket steric hindrance to CN^- binding properties in *Tt* H-NOX. Using this model, the CN^- binding properties of additional mutants (F78V and F78Y) are predicted and tested. All mutants have spectral changes that linearly correspond to cyanide concentration and all of them show better anion selectivity than the WT analogue. As predicted, F78V binds cyanide with the highest affinity.

(23) Pellicena, P.; Karow, D. S.; Boon, E. M.; Marletta, M. A.; Kuriyan, J. *Proc. Natl. Acad. Sci. U.S.A.* **2004**, *101*, 12854.
(24) Zhao, Y.; Brandish, P. E.; Ballou, D. P.; Marletta, M. A. *Proc. Natl. Acad. Sci. U.S.A.* **1999**, *96*, 14753.
(25) Karow, D. S.; Pan, D.; Tran, R.; Pellicena, P.; Presley, A.; Mathies, R. A.; Marletta, M. A. *Biochemistry* **2004**, *43*, 10203.
(26) Boon, E. M.; Huang, S. H.; Marletta, M. A. *Nat. Chem. Biol.* **2005**, *1*, 53.
(27) Olea, C.; Boon, E. M.; Pellicena, P.; Kuriyan, J.; Marletta, M. A. *ACS Chem. Biol.* **2008**, *3*, 703.
(28) Dai, Z.; Boon, E. M. *J. Inorg. Biochem.*, submitted for publication, 2010.
(29) Boon, E. M.; Marletta, M. A. *J. Am. Chem. Soc.* **2006**, *128*, 10022.

Materials and Methods

Protein Expression and Purification. Plasmids for 6×His tagged WT and P115A *Tt* H-NOX were generated in previous studies.[28] *Tt* H-NOX mutagenesis was carried out using a QuikChange mutagenesis kit (Stratagene). The primers used to generate the F78V mutant were 5′-ggaaggcagaacataaaaactgtcagcgaatggtttccctcc-3′ and its reverse complement. The primers used to generate the F78Y mutant were 5′-ggaaggcagaacataaaaacttacagcgaatggtttccctcc-3′ and its reverse complement. Expression, purification, and storage of all H-NOX proteins were carried out as previously described.[28]

Cyanide Detection. All cyanide quantification and ligand binding affinity experiments were carried out in 50 mM HEPES buffer, pH 7.5, at 20 °C unless otherwise noted. The KCN solutions were prepared freshly before use. All UV/visible spectra were obtained using a Cary 100 Bio Spectrophotometer (Varian, now Agilent Technologies) equipped with a constant temperature bath.

All WT and mutant *Tt* H-NOX proteins discussed here are in their ferric states. In a typical cyanide detection experiment, *Tt* H-NOX ferric protein was produced by oxidizing the protein with 15−100 mM potassium ferricyanide; excess potassium ferricyanide and product ferrocyanide were removed by desalting through a PD-10 column (GE Healthcare). After desalting, protein concentration was measured based on its UV/visible absorbance (Beer−Lambert law). Next, separate equal volume samples of the protein with varying cyanide concentration, from 0 μM to more than twice the concentration of the sensor protein, were prepared. After the binding reached equilibrium (samples were monitored until there was no further spectral change), final UV/visible spectra for all samples were taken. Excel (Microsoft) was used to generate difference absorption spectra by subtracting the spectrum of the protein without cyanide from each spectrum with cyanide. Origin 7.0 was utilized to plot and fit the absorbance changes in the Soret and α/β band region, as well as the Soret band maximum, versus cyanide concentration.

Anion Selectivity Assay. To study the anion selectivity of *Tt* H-NOX and mutants as cyanide sensors, excess amounts (100 equiv anions for WT and 200 equiv anions for P115A) of potential interfering anions, including SO_4^{2-} (Na_2SO_4), AcO^- (NaOAc), HCO_3^- ($NaHCO_3$), F^- (NaF), Cl^- (NaCl), Br^- (NaBr), I^- (NaI), NO_3^- ($NaNO_3$), $C_2O_4^{2-}$ ($Na_2C_2O_4$), ClO_4^- ($KClO_4$), SCN^- (NaSCN), phosphate (NaH_2PO_4), and EDTA (sodium salt), were added to *Tt* H-NOX solutions, separately, both in the presence and absence of cyanide. UV/visible spectra of all samples were taken to assess anion binding. To test the selectivity of P115A *Tt* H-NOX as a colorimetric probe, digital photographs were also taken after 10 min following the addition of various anions.

Cyanide and Fluoride Equilibrium Dissociation Constants. Spectrophotometric equilibrium titrations of *Tt* H-NOX ferric proteins with cyanide or fluoride were performed at 20 °C using UV/visible spectroscopy as described above. Difference spectra were calculated by subtracting the first scan (the sample with 0 mM anion) from subsequent scans (samples with increasing anion amount). The equilibrium dissociation constants (K_D) of all proteins for CN^- and F^- were determined by plotting maximal absorbance

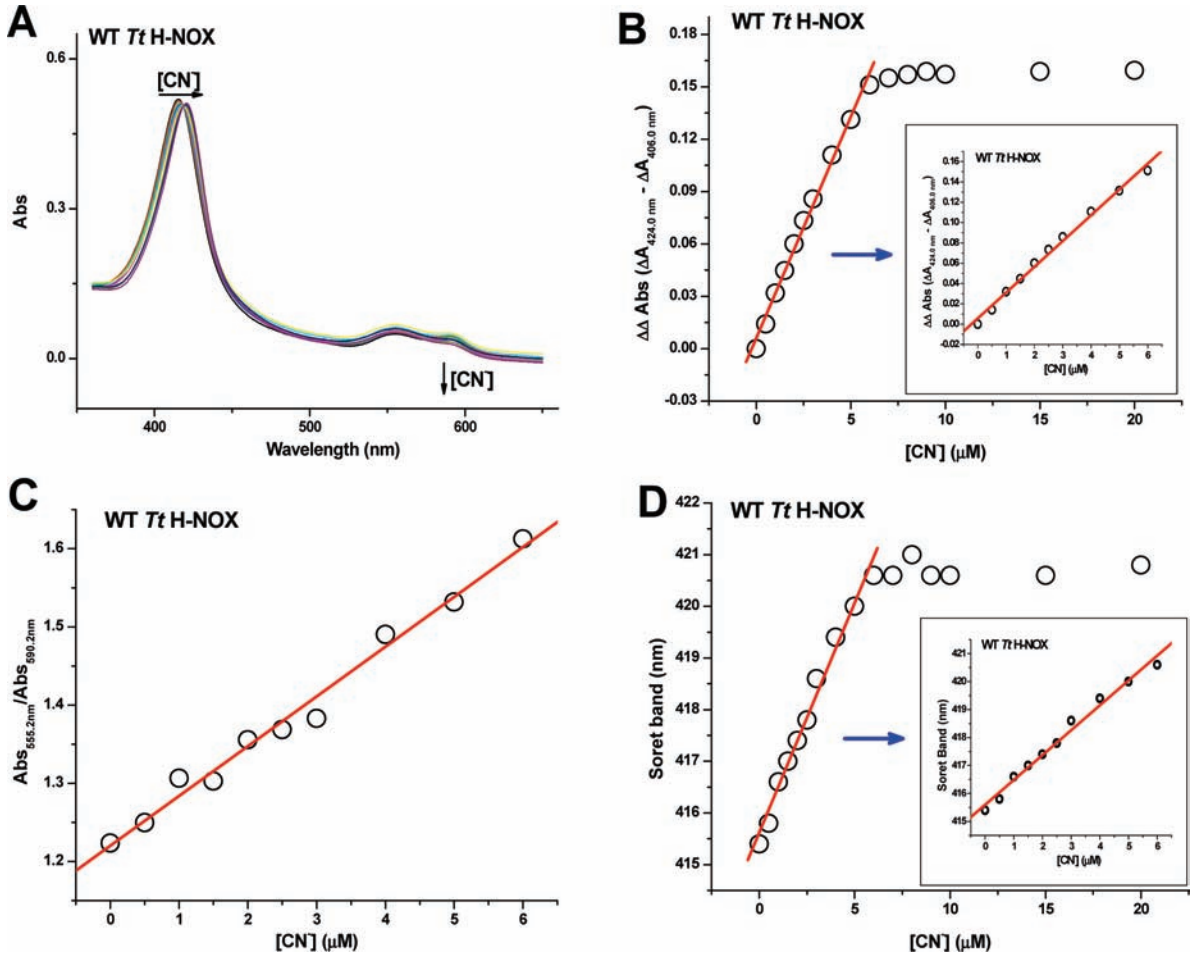

Figure 2. Quantification of cyanide using 6 μM WT *Tt* H-NOX. (A) UV/visible spectral shifts upon cyanide addition. Cyanide can be sensitively detected using multiple spectroscopic features. Cyanide detection based on absorbance changes in the Soret band region (B), absorbance changes in the β/α band region (C), and the Soret band maximum shift (D). $R^2 = 0.99$ for each line.

difference for each scan versus anion concentration and curve fitting with the following equation:[30]

$$\Delta A = \Delta A_{max}([P] + [L] + K_D - (([P] + [L] + K_D)^2 - 4[P][L])^{1/2})/2[P] \quad (1)$$

Here ΔA is the absorbance difference; ΔA_{max} is the maximum absorbance difference when all the ferric heme molecules are occupied with anion; [P] and [L] are the total protein and total anion concentration, respectively; and K_D is the equilibrium dissociation constant.

Results and Discussion

Simple and inexpensive techniques for cyanide detection and quantification at the submicromolar level are required. *Tt* H-NOX detects CN^- at the 10 ppb level and affords multiple handles for cyanide sensing, including visual detection, which makes it unique compared to other small-molecule probes. Further, cyanide sensing can be fine-tuned by rational engineering of the H-NOX heme pocket.

***Tt* H-NOX Is a Sensitive and Selective CN^- Sensor.** We first investigated the quantification of cyanide with WT *Tt* H-NOX. Cyanide was added to 6 μM ferric WT *Tt* H-NOX solutions to final concentrations of 0−20 μM. The binding reached equilibrium within 75 min at 20 °C, and when the temperature was increased to 37 °C, the reaction time decreased to 45 min. Because *Tt* H-NOX is a thermostable protein, we can further increase the cyanide association rate and shorten the reaction time using temperature.

UV/visible spectroscopy of *Tt* H-NOX in reaction with varying concentrations of CN^- revealed that, with increasing cyanide concentration (until ~6 μM, the concentration of H-NOX in the reaction), the Soret band shifts from 415.4 to 420.6 nm (Figure 2A), which is attributed to the replacement of a water molecule with cyanide at the distal binding site of the heme pocket. We plotted the change in absorbance of ferric WT *Tt* H-NOX upon cyanide addition verses cyanide concentration and obtained a good linear relationship until the concentration of cyanide exceeded the concentration of the sensor (6 μM), implying strong, one-to-one binding (Figure 2B). We also found that the β/α absorbance band ratio linearly correlates with cyanide concentration (Figure 2C). Interestingly, we observed a linear response in the Soret band maximum as a function of cyanide concentration (from 0 to 6 μM), which indicates that we can quantify cyanide in an unknown sample simply based on reading the Soret band maximum from the UV/visible spectrum (Figure 2D).

The detection limit is as low as 0.5 μM with a detection range of 0−6 μM in this assay. We can broaden the detection range by increasing the sensor concentration since CN^- binding is

(30) Bidwai, A.; Witt, M.; Foshay, M.; Vitello, L. B.; Satterlee, J. D.; Erman, J. E. *Biochemistry* **2003**, *42*, 10764.

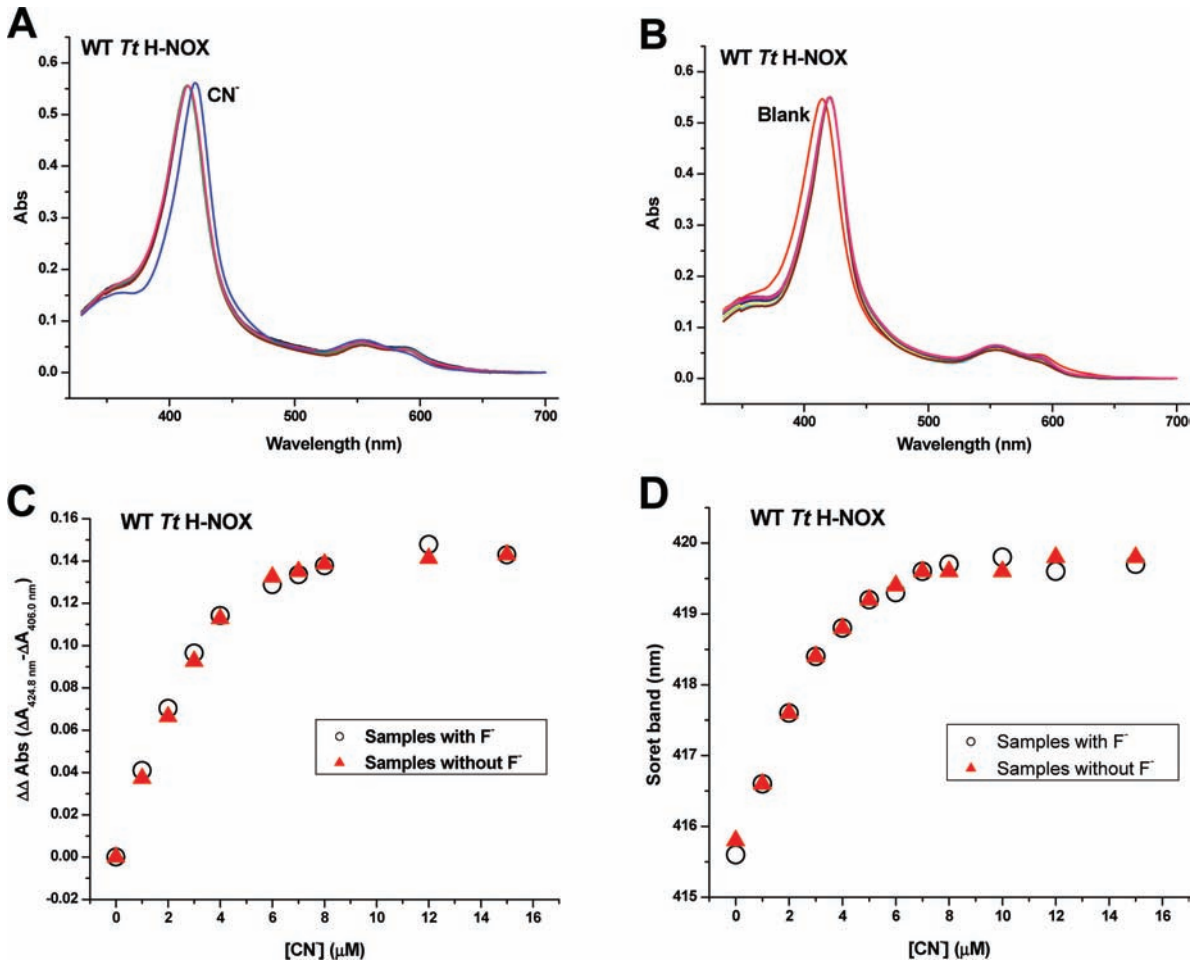

Figure 3. Anion selectivity of WT *Tt* H-NOX. (A) Spectra of WT *Tt* H-NOX (6 μM) after the addition of buffer only (blank) and 600 μM SO_4^{2-}, AcO^-, HCO_3^-, F^-, Cl^-, Br^-, I^-, NO_3^-, $C_2O_4^{2-}$, ClO_4^-, SCN^-, phosphate, EDTA, or CN^-. Only the cyanide sample (blue curve) yields a typical red-shift and the fluoride sample gives a ~0.4 nm blue-shift. (B) Spectra of WT *Tt* H-NOX (6 μM) after adding cyanide (6 μM) to samples in the presence of various existing anions (from above). All samples give typical cyano−complex spectra and only the blank sample (red curve), to which no CN^- was added, yields no spectral change. (C) Soret band absorbance change and (D) Soret band maximum shift of WT *Tt* H-NOX (6 μM) upon the addition of cyanide (0−15 μM) with and without the presence of 100 equiv of fluoride (600 μM).

one-to-one with respect to protein. We repeated this experiment using 30 μM ferric WT *Tt* H-NOX. As expected, we found that the Soret band and β/α band ratio are both linearly correlated with the cyanide concentration to as much as 30 μM (Figures S1 and S2), which is described as the necessary cyanide monitoring range for human physiological safeguard.[5] These multiple sensing features, especially the direct cyanide quantification based on the Soret band maximum, render *Tt* H-NOX an excellent candidate for cyanide detection and quantification.

To examine the selectivity of WT *Tt* H-NOX, 100 equiv (600 μM) of various anions, including SO_4^{2-}, AcO^-, HCO_3^-, F^-, Cl^-, Br^-, I^-, NO_3^-, $C_2O_4^{2-}$, ClO_4^-, SCN^-, phosphate, and EDTA, were added separately to the sensor solution (6 μM). None of the anions tested caused a change to the spectrum of WT *Tt* H-NOX, except for F^- (Figure 3A). Weak binding of F^- to the ferric heme brought about a small but consistent blue shift (~0.4 nm) to the Soret band maximum. Cyanide was then added (6 μM) to each anion test sample, which caused the Soret band in each sample (including the F^- sample) to shift to 420.6 nm, indicative of formation of the $Fe^{3+}-CN^-$ complex (Figure 3B).

Next, we examined WT *Tt* H-NOX cyanide quantification in the presence of 100 equiv of F^- and found that excess F^- does not affect CN^- quantification based on absorbance change measurements (Figure 3C and Figure S3). We did not observe any interference from fluoride during quantification by the Soret band maximum shift until the amount of F^- was ~1000 times greater than CN^- (Figure S4).

Finally, we measured the equilibrium dissociation constants (K_D) for CN^- and F^- binding to WT *Tt* H-NOX (Figures S5 and S6). As listed in Table 1, WT *Tt* H-NOX has a K_D for F^- of 3.5 mM, which is much larger than its K_D for CN^- of 80 nM. This difference explains the high tolerance toward fluoride during cyanide detection.

The *Tt* H-NOX P115A Mutant Is a Colorimetric CN^- Sensor. A colorimetric sensor would be desirable for cyanide detection. Because of lack of a requirement for sophisticated equipment, such a sensor would be ideal for employment in the field. We did not see a color change in the wild-type sensor upon the addition of cyanide. However, it has been found that changes in the solvent properties can improve the visual detection of cyanide by small molecule sensors;[9] therefore, we hypothesized that an alteration at the cyanide sensing site may introduce a color change and render *Tt* H-NOX as a sensor for visual cyanide detection. Hence, the cyanide sensing properties were investigated for a previously characterized *Tt* H-NOX mutant, P115A.

Table 1. Ligand Binding Properties of *Tt* H-NOX Proteins

	Soret band (nm)				
sensor	$Fe^{3+}-H_2O$	$Fe^{3+}-CN^-$	$K_{D\,(CN^-)}$ (M)	$K_{D\,(F^-)}$ (M)	$K_{D\,(CN^-)}/K_{D\,(F^-)} \times 10^{-6}$
WT	415.4	420.6	$(8 \pm 2) \times 10^{-8}$	$(3.5 \pm 0.2) \times 10^{-3}$	23
P115A	405.0	420.0	$(29 \pm 11) \times 10^{-8}$	N/A[a]	N/A
F78V	414.5	420.0	$(1.6 \pm 0.9) \times 10^{-8}$	$(3.93 \pm 0.05) \times 10^{-3}$	4
F78Y	414.6	420.0	$(46 \pm 11) \times 10^{-8}$	$(33.1 \pm 0.3) \times 10^{-3}$	14

[a] As F^- induces no spectral changes to P115A, its K_D value is not measurable.

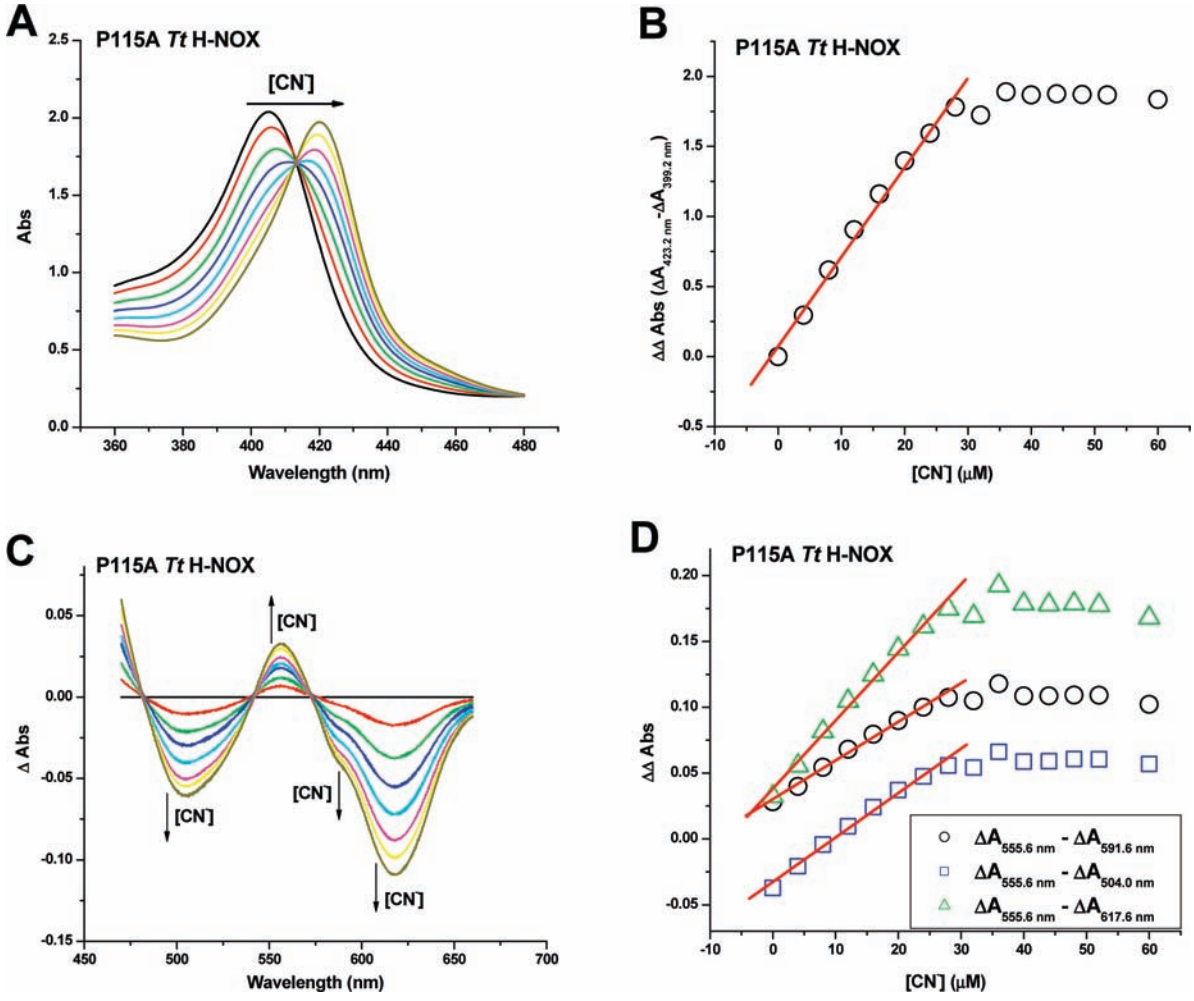

Figure 4. Quantification of cyanide using 20 μM P115A *Tt* H-NOX protein. UV/visible spectral changes at the Soret band region (A) and the β/α band region (C) upon the addition of cyanide. Cyanide can be sensitively detected using multiple spectroscopic features. Cyanide detection based on absorbance changes at the Soret band region (B) and the β/α band region (D). $R^2 = 0.99$ for each line.

Proline 115 sits very close to the heme in the proximal heme pocket of *Tt* H-NOX (Figure 1) causing the heme to distort (saddling and ruffling distortions).[23] On the basis of crystallographic and spectroscopic characterization,[27] the P115A *Tt* H-NOX mutation alters the conformation of the heme, making it less distorted than wild-type and causing a shift in one of the helices in the distal heme pocket. The structure and some biochemical properties of ferrous complexes of *Tt* H-NOX P115A have been previously reported.[27] In particular, P115A has been demonstrated to cause a shift in the redox potential of *Tt* H-NOX, compared to WT.[27] We hypothesized these changes in the electronic environment of the CN^- binding site might alter the CN^- sensing attributes of *Tt* H-NOX, analogously to changing the solvent with a small molecule CN^- sensor.[9]

To test the CN^- sensing properties of P115A *Tt* H-NOX, 20 μM P115A was incubated with 0−60 μM CN^- and the binding reaction was monitored by UV/visible spectroscopy (Figure 4). Like WT, the absorbance changes in Soret band region and β/α band region all linearly respond to cyanide concentration, which affords multiple parameters to quantify CN^- in a variable range dictated by the H-NOX concentration. We noticed that, upon CN^- binding, P115A yields a much larger Soret band maximum shift (from 405.0 to 420.0 nm) and more dramatic changes in the α/β band region (Figure 4A,C), implying that it could be an even better cyanide sensor than the WT *Tt* H-NOX.

Importantly, we observed a color change from dark brown to bright orange after adding cyanide for 10 min (Figure 5, top panel), which enables us to visually detect cyanide and also confirms our hypothesis that we can improve this cyanide sensing system by modifying the *Tt* H-NOX heme pocket. This color change is possible because P115A H-NOX is dark brown in the $Fe^{3+}-OH_2$ state, while WT $Fe^{3+}-OH_2$ and all of the *Tt*

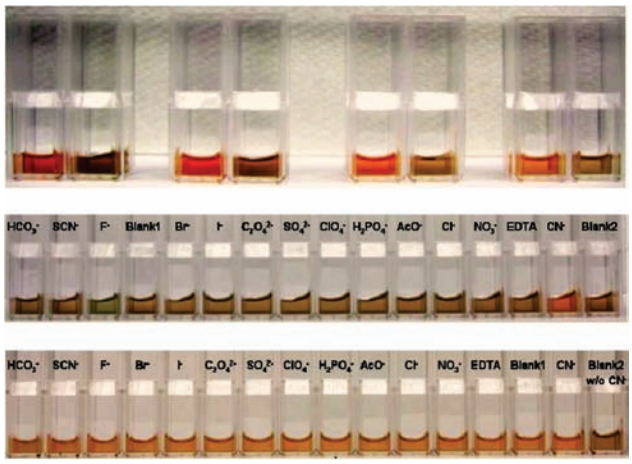

Figure 5. Selective visual detection of cyanide using P115A *Tt* H-NOX. (Top panel) Color change of P115A *Tt* H-NOX upon CN^- binding. From left to right: 120, 100, 80, and 60 μM P115A *Tt* H-NOX with and without 2 equiv of CN^-. (Middle panel) 14 different anions (at 15 mM) were added to 75 μM P115A *Tt* H-NOX. Blank 1 and 2 contain only protein. (Bottom panel) CN^- (150 μM) was added to each sample from above except blank 2. Only cyanide changes the color of the protein from dark brown to orange.

H-NOX $Fe^{3+}-CN^-$ complexes are orange in color. This difference in the electronic structure of P115A is likely caused by the flattened heme in the P115A mutant, as discussed above.[27] The change in redox potential may also contribute to the introduction of colorimetric cyanide detection with the P115A mutation.

Furthermore, we found that P115A *Tt* H-NOX has similar CN^- sensitivity and better anion selectivity than WT *Tt* H-NOX. Anion selectivity tests (anion concentration 15 mM) with P115A *Tt* H-NOX (75 μM) revealed that only CN^- changes the UV/visible spectrum (Figure 6A) and only CN^- changes the color of P115A *Tt* H-NOX from brown to orange (Figure 5, middle panel). Even with a large excess of F^- (15 mM), we found no measurable detection of F^- binding based on UV/visible absorption changes. We need to point out that F^- brings about a very slight visually detectable color change, toward green in the absence of CN^-, but this does not affect cyanide detection. After adding cyanide (150 μM) to each sample containing the various competing anions, we observed spectra typical of the CN^--bound complex (Figure 6B) as well as the expected brown-to-orange color change for all samples (Figure 5, bottom panel). Furthermore, from our studies, a color change is detectable at $\sim$25 μM CN^- (Figure S7) with 75 μM P115A *Tt* H-NOX.

The K_D value of cyanide binding to P115A was determined to be 290 nM (Table 1 and Figure S5). Although P115A binds CN^- less tightly than WT, the addition of a color change, and lack of F^- binding, make it an attractive construct for cyanide sensing.

On the basis of our recent X-ray absorption spectroscopy results,[28] during the replacement of water with CN^- at the heme pocket, the central iron in P115A *Tt* H-NOX experiences a larger shift toward the distal pocket (0.16 Å) than the iron for WT (0.06 Å). As a result, while the iron in the WT *Tt* H-NOX $Fe^{3+}-CN^-$ complex is located almost exactly at the center of the porphyrin nitrogens, the iron in the P115A *Tt* H-NOX $Fe^{3+}-CN^-$ complex moves into the distal pocket. We measured the iron shift upon ligation for a range of ferrous and ferric complexes of both WT and P115A *Tt* H-NOX and found the most dramatic shift toward the distal pocket with the $Fe^{3+}-CN^-$ complex of P115A. Thus, in addition to an altered heme conformation, the P115A mutation leads to a more crowded distal pocket for the $Fe^{3+}-CN^-$ complex of *Tt* H-NOX. The more crowded ligand binding cavity causes more steric strain in the $Fe^{3+}-CN^-$ complex of P115A than WT. This strain destabilizes the CN^- complex, which explains the larger K_D for $Fe^{3+}-CN^-$ in P115A.

Cyanide Detection Properties of *Tt* H-NOX Can Be Rationally Engineered through Mutation. Our results with P115A led us to the hypothesis that distal pocket crowding is a key feature for CN^- affinity using *Tt* H-NOX. In support of our hypothesis, it has previously been demonstrated that steric hindrance from the distal residues of heme pocket can perturb ligand binding to hemoproteins.[31,32]

To directly test our hypothesis relating distal pocket crowding to CN^- binding properties, we selected phenylalanine 78 for mutation. F78 is in the distal pocket, packed against the heme, with its benzyl group directed toward the exogenous ligand binding site (Figure 1). Therefore, we

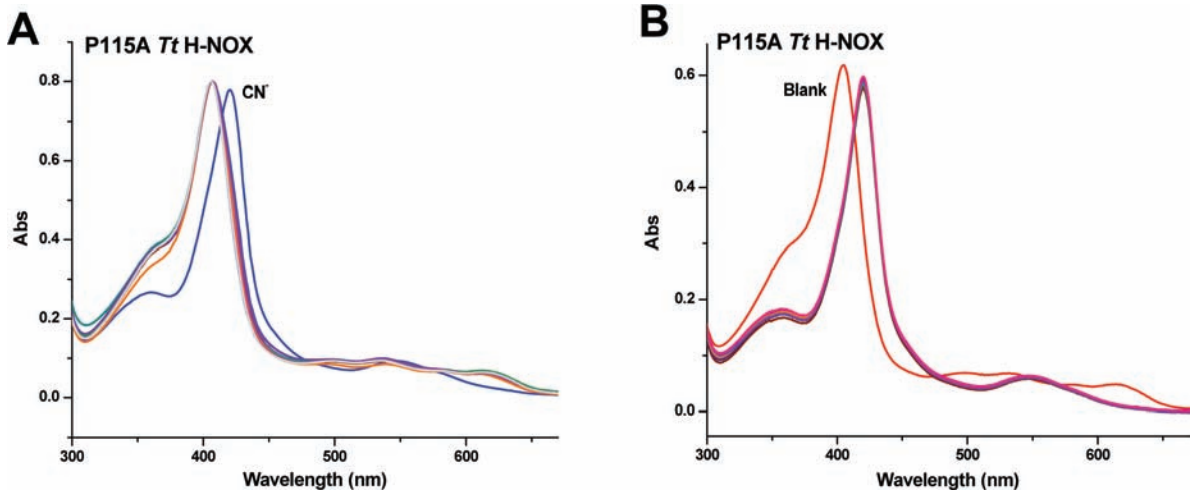

Figure 6. (A) Spectra of P115A *Tt* H-NOX (75 μM) after the addition of buffer only (blank) and 15 mM SO_4^{2-}, AcO^-, HCO_3^-, F^-, Cl^-, Br^-, I^-, NO_3^-, $C_2O_4^{2-}$, ClO_4^-, SCN^-, phosphate, EDTA, or CN^-. Only the cyanide sample (blue curve) yields a spectral shift. (B) Spectra of P115A *Tt* H-NOX (75 μM) after adding cyanide (150 μM) to samples in the presence of various existing anions (from above). All samples give typical cyano−complex spectra and only the blank sample (red curve), to which no CN^- was added, yields no spectral change.

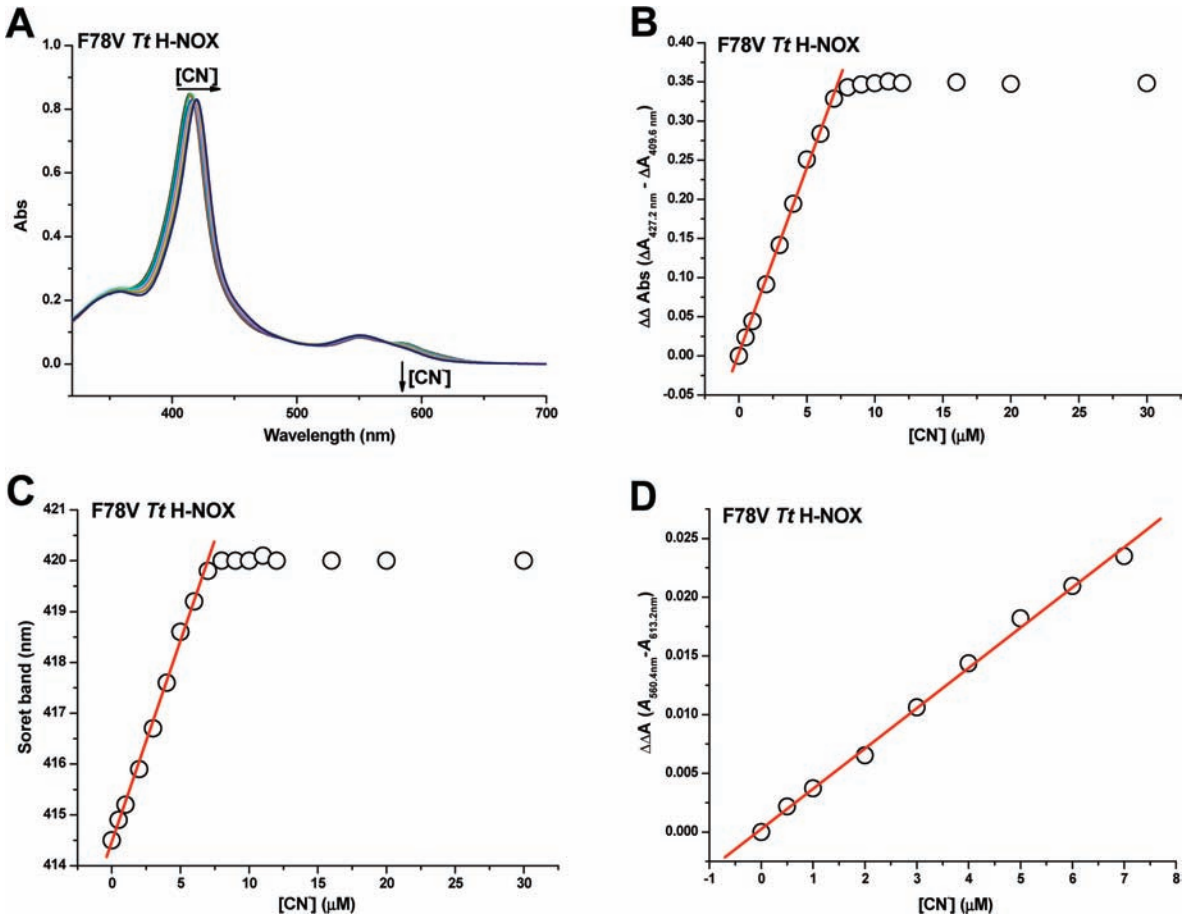

Figure 7. Quantification of cyanide using 7 μM F78V *Tt* H-NOX. (A) UV/visible spectral changes upon the addition of cyanide. Cyanide detection based on absorbance changes at the Soret band region (B), the β/α band region (D), and based on Soret band maximum shift (C). $R^2 = 0.99$ for each line.

hypothesized that adjusting the size of cyanide binding pocket by changing this residue should affect the cyanide sensing features. Using site-directed mutagenesis, we obtained two mutants, F78V with a less crowded distal pocket, and F78Y with a more crowded distal pocket.

Like all other *Tt* H-NOX constructs, the absorption spectral changes in both the Soret band and β/α band regions titrate with cyanide concentration for both F78V and F78Y (here 0−30 μM CN^- was incubated with 7 μM F78V and 0−20 μM CN^- was incubated with 8 μM F78Y). Similarly, we can also quantify the amount of cyanide present in a sample using the Soret band position, as it shifts from 414.5 to 420.0 nm linearly with increasing CN^-. Thus, [CN^-] can be quantified using the Soret band maximum position or absorption changes (Figures 7 and 8).

More importantly, as shown in Table 1 and Figure S5, the cyanide binding affinity for F78V is increased by ~5-fold compared with WT, which makes this mutant the tightest CN^- receptor among all proteins tested here. Moreover, the F^- affinity is decreased slightly (Table 1 and Figure S6), and thus, the synergistic effect leads to a large increase in the selectivity of cyanide over fluoride [$K_D(CN^-)/K_D(F^-) = 4 \times 10^{-6}$; Table 1] compared to WT. Removal of the F78 benzyl side chain from the distal pocket likely creates an emptier cyanide binding pocket. The less crowded pocket leads to stabilization of the cyano-complex by providing extra space to help release the steric strain caused by the binding of cyanide and movement of iron toward the distal side.

F78Y, in contrast, interferes with the binding of anions. The affinities for cyanide and fluoride are decreased by ~6- and ~10-fold, respectively (Table 1 and Figures S5 and S6) in comparison to WT, and the net effect is an increase in anion selectivity in F78Y mutant. F78Y, in addition to increasing steric bulk, also introduces an additional possible hydrogen bond for CN^-. However, apparently the destabilization from steric interference overwhelms the effect of a potentially stabilizing H-bonding, as F78Y has a significantly larger equilibrium dissociation constant for CN^- binding. The CN^- binding affinity changes in F78V and F78Y mutant proteins support our hypothesis linking steric bulk with CN^- affinity. More importantly, the data presented here suggest that *Tt* H-NOX can be further tuned for cyanide sensing.

Conclusion

Tt H-NOX is a novel cyanide sensing system with high selectivity and excellent sensitivity. With this simple and straightforward cyanide sensing technique, we have achieved a cyanide detection limit as low as 0.5 μM. The linear response to cyanide of multiple probing features, especially the Soret band maximum shift, renders this detection

(31) Balasubramanian, S.; Lambright, D. G.; Boxer, S. G. *Proc. Natl. Acad. Sci. U.S.A.* **1993**, *90*, 4718.
(32) Rodriguez-Lopez, J. N.; Smith, A. T.; Thorneley, R. N. F. *J. Biol. Chem.* **1997**, *272*, 389.

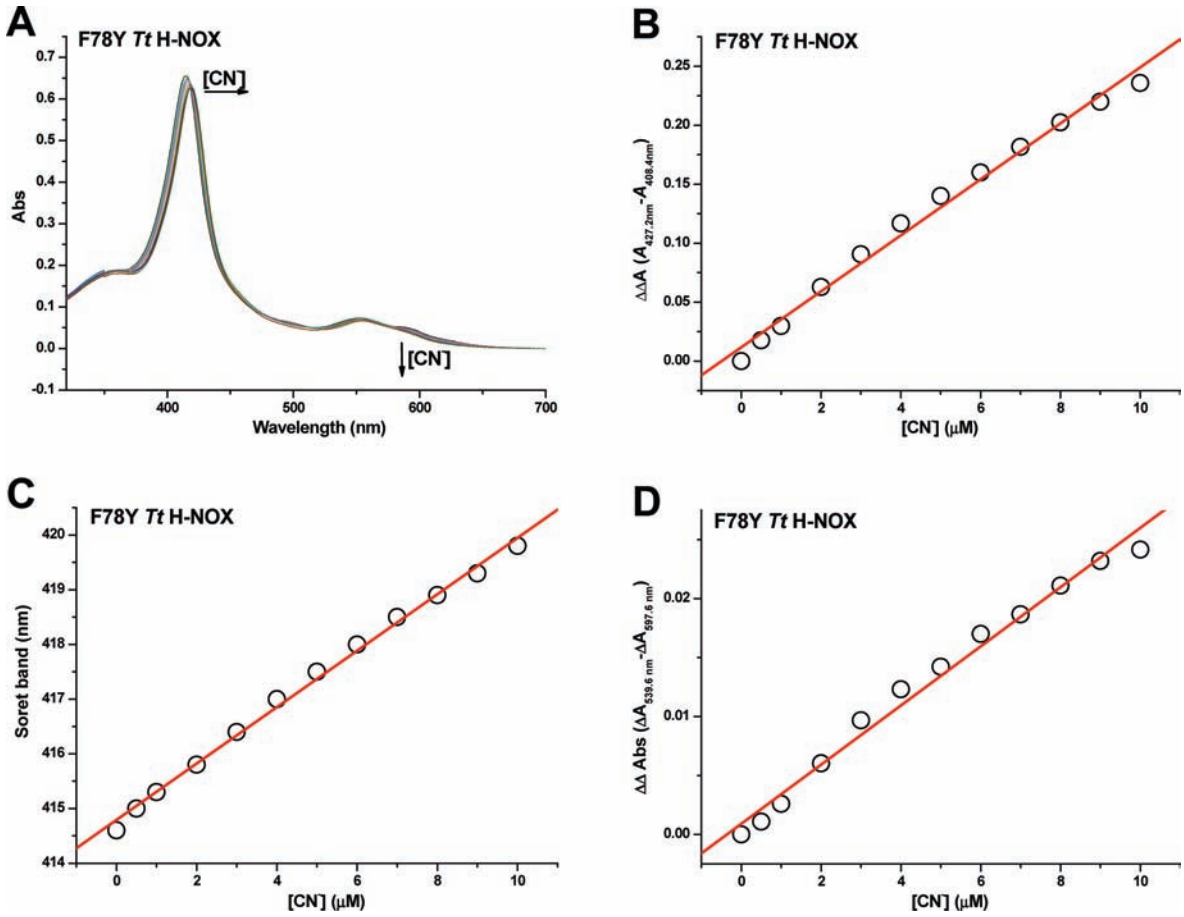

Figure 8. Quantification of cyanide using 8 μM F78Y *Tt* H-NOX. (A) UV/visible spectral changes upon the addition of cyanide. Cyanide detection based on absorbance changes at the Soret band region (B), the β/α band region (D), and based on Soret band maximum shift (C). $R^2 = 0.99$ for each line.

technique unique compared to other cyanide sensing schemes. Furthermore, we have shown that we can improve this system through modifying the heme pocket. We were able to introduce colorimetric detection and enhance anion selectivity in ferric P115A *Tt* H-NOX. Through replacing F78 with a smaller (valine) or a bigger residue (tyrosine), we tuned the binding affinity of cyanide and improved the anion selectivity. In particular, the F78V protein shows a significant increase in CN^- binding affinity and selectivity. The sensitivity of *Tt* H-NOX to CN^-, in addition to the extreme stability of *Tt* H-NOX, its tolerance of excess anions, and its independent of organic solvents, make it a practical sensor for cyanide monitoring.

Acknowledgment. This work was supported by New York State Foundation for Science, Technology and Information grant C060030 to E.M.B., National Science Foundation grant CHE-0910771 to E.M.B., and Stony Brook University.

Supporting Information Available: Cyanide quantification and fluoride interference studies with *Tt* H-NOX WT. K_D measurement for CN^- and F^- binding. Visual CN^- detection. This material is available free of charge via the Internet at http://pubs.acs.org.

JA101674Z